

Chaos and reliability in balanced spiking networks

Guillaume Lajoie¹, Kevin K. Lin², Eric Shea-Brown¹

¹University of Washington, Dept. of Applied Mathematics; ²University of Arizona, Dept. of Mathematics

The question of reliability arises for any dynamical system driven by an input signal: if the same signal is presented many times with different initial conditions, will the system entrain to the signal in a repeatable way? Reliability is of particular interest in large, randomly coupled networks of excitatory and inhibitory units. Such networks are ubiquitous in neuroscience, but are known to autonomously produce strongly chaotic dynamics – an obvious threat to reliability. Here, we show that such chaos also occurs in the presence of weak and strong stimuli. However, even in the chaotic regime, intermittent periods of highly reliable spiking often coexist with unreliable activity. We argue that the sustained coexistence of chaos and reliable spike events is due to the interaction of global state space expansion and dynamics local to individual cells, and interpret our findings within the framework of random dynamical systems theory.

Reliability is a general property of dynamical systems driven by input signals. This refers to the reproducibility of a system’s output on many trials, where the same driving signal is presented but initial system states vary. The concept is fundamental in neuroscience: for a network of interacting cells receiving sensory and internal stimuli, the degree to which it is reliable impacts its ability to encode information via precise temporal spike patterns. Related phenomena arise in a variety of physical and engineered systems, including coupled lasers [1] and coupled chaotic systems [2]. Understanding the conditions and dynamical mechanisms that govern network reliability stands as a broad challenge in the study of networks of dynamical systems.

The question of reliability is of particular relevance for an ubiquitous and important class of neural networks, those with a balance of excitatory and inhibitory connections [3]. Such *balanced networks* produce dynamics that match the irregular firing observed experimentally on the “microscale” of single cells, and on the macroscale have rapid and linear mean-field dynamics that could be beneficial for neural computation [4–8]. However, such balanced networks are known to produce strongly chaotic activity when they fire autonomously or with constant inputs [6, 8, 9]. On the surface, this appears incompatible with reliable spiking, as small differences in initial conditions between trials may lead to very different responses. However, that the answer might be more subtle is suggested by a variety of results on the impact of temporally fluctuating inputs on chaotic dynamics [10–16].

In this Letter, we present a detailed numerical study and steps toward a qualitative theory of reliability in fluctuation-driven balanced networks. We explore the relationship between the Lyapunov spectrum, which quantifies the average stability of trajectories on long timescales, and the cross-trial repeatability of spike times over shorter timescales. Even in the presence of positive Lyapunov exponents, we find that spike times can display sharp temporal precision from trial to trial. These reliable spike events are interspersed with more diffuse spiking, in which spike times are impacted by prior net-

work states differing from trial to trial. Thus, networks with positive Lyapunov exponents produce two types of spike events, representing either inputs alone or a combination of inputs and past network states.

Model and single-trial dynamics: We study a temporally driven network of $N = 1000$ spiking neurons. Each neuron is modeled by a phase variable $\theta_i \in S^1 = \mathbb{R}/\mathbb{Z}$ whose dynamics follow the “ θ -neuron” model [17], capturing the saddle-node on an invariant circle (SNIC) bifurcation responsible for spike generation in Type I neurons. These dynamics are equivalent to the quadratic integrate-and-fire (QIF) model after a change of coordinates [18]. The underlying “normal form” dynamics [19] are found in many brain areas and are known to produce reliable responses to stimuli in isolated cells [13, 20], cf. [21, 22]. Thus, any unreliability or chaos that we find is purely a consequence of network interactions.

Coupling from neuron j to neuron i is determined by the weight matrix $A = \{a_{ij}\}$. A is chosen randomly using an Erdős-Renyi scheme such that 20% of the cells j are inhibitory ($a_{ij} < 0 \forall i$) and 80% are excitatory ($a_{ij} > 0 \forall i$); we do not allow self-connections, setting $a_{ii} = 0$. Each neuron has *mean* in-degree $K = 20$ from each population (excitatory and inhibitory) and the synaptic weights are $\mathcal{O}(1/\sqrt{K})$ in accordance with the classical balanced-state network architecture [6]. We note that our results appear to be qualitatively robust to changes in N and K , but a detailed study of scaling limits is beyond the scope of this paper.

A neuron j is said to fire a spike when $\theta_j(t)$ crosses $\theta_j = 1$; when this occurs, θ_i is impacted via the coupling term $a_{ij}g(\theta_j)$ where $g(\theta)$ is a smooth “bump” function with small support ($[-1/20, 1/20]$) around $\theta = 0$ satisfying $\int_0^1 g(\theta)d\theta = 1$, meant to model the rapid rise and fall of a pulsatile synaptic variable. In addition to coupling interactions, each cell receives a stimulus $I_i(t) = \eta + \varepsilon\zeta_i(t)$ where η represents a constant current and $\zeta_i(t)$ are independent white noise processes, scaled by the amplitude parameter ε . Here, $\zeta_i(t)$ represents a “frozen” (quenched), aperiodic signal (as in [13, 21, 22]).

The i^{th} neuron in the network is therefore described

by the following SDE:

$$d\theta_i = [F(\theta_i) + Z(\theta_i) \left(\eta + \sum_j a_{ij} g(\theta_j) \right) + \frac{\varepsilon^2}{2} Z(\theta_i) Z'(\theta_i)] dt + \varepsilon Z(\theta_i) dW_{i,t} \quad (1)$$

where the intrinsic dynamics $F(\theta_i) = 1 + \cos(2\pi\theta_i)$ and the stimulus response curve $Z(\theta_i) = 1 - \cos(2\pi\theta_i)$ come directly from coordinate changes from the original QIF equations (see Supplemental Materials (SM) [23] and [17]). Here, $W_{i,t}$ is the independent Wiener process generating $\zeta_i(t)$; the ε^2 term is the Itô correction from the coordinate change [24]. Finally, η sets the intrinsic excitability of individual cells. For $\eta < 0$, there is a stable and an unstable fixed point, together representing resting and threshold potentials. Thus (contrasting [8] where cells are intrinsically oscillatory), cells are in the “excitable regime,” displaying *fluctuation-driven* firing, as for many cortical neurons [25].

Fig. 1 illustrates that the general properties of the network dynamics, including a wide distribution of firing rates from cell to cell and highly irregular firing in individual cells, are consistent with many balanced-state networks from the literature as well as general observations from cortex [4, 5]. Furthermore, the network’s mean firing rate scales monotonically with η and ε (not shown) as in [6, 8].

Asymptotic reliability: We say a network is *asymptotically reliable* if for any fixed input signal (a realization of $\zeta(t) = \{\zeta_i(t)\}_{i=1\dots N}$), solutions starting with distinct initial conditions (ICs) converge to a single trajectory,

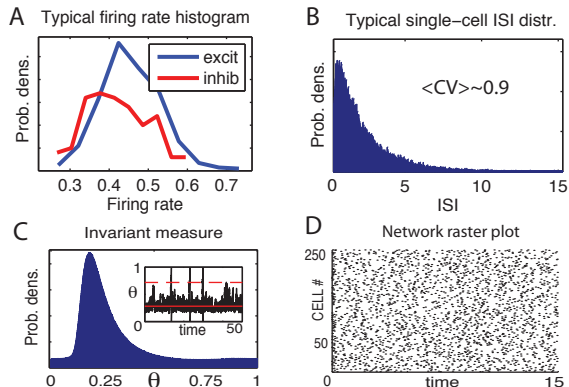


FIG. 1. (A) Typical firing rate distributions for excitatory and inhibitory populations. (B) Typical inter-spike-interval (ISI) distribution of a single cell. The coefficient of Variation (CV) is close to 1. (C) Invariant measure for an excitable cell ($\eta < 0$); inset: typical trajectory trace of an excitable cell where solid and dotted lines mark the stable and unstable fixed points. (D) Network raster plots for 250 randomly chosen cells. For all panels, $\eta = -.5$, $\varepsilon = 0.25$.

therefore producing spikes at the same precise time on every trial.

In this context, it is useful to treat (1) as a random dynamical system (RDS) on \mathbb{T}^N . That is, we view the system as a nonautonomous ODE driven by a frozen realization of $\zeta(t)$, and consider the action of the generated family of flow maps on phase space. For such a RDS, Lyapunov exponents $\lambda_1 \geq \lambda_2 \geq \dots \geq \lambda_N$ are well defined and are constant for almost every choice of $\zeta(t)$ and almost every IC. Assuming a number of nondegeneracy conditions, it can be shown [26, 27] that when $\lambda_1 < 0$, almost every trajectory will converge to a *random sink*: a ζ -dependent, asymptotically stable trajectory on \mathbb{T}^N . We note that although deterministic systems tend to have multiple basins with $\lambda_1 < 0$, RDS’s often have a single random sink because of ergodicity (see SM [23]). On the other hand if $\lambda_1 > 0$, solutions are attracted to *random strange attractors* [28] (called “snapshot attractors” in [29]). These are time-dependent versions of *Sinai-Ruelle-Bowen measures* for dissipative chaotic systems [30], and often are not localized in state space. We therefore use the sign of λ_1 as an indicator of the asymptotic reliability of the network (1). That is, if $\lambda_1 < 0$, we expect almost every solution to converge to a unique trajectory whereas if $\lambda_1 > 0$, this is a strong indication that dynamics are chaotic and thus not asymptotically reliable.

In Fig. 2 (A) we present the dependence of the first 100 Lyapunov exponents for a network with fixed mean input $\eta = -0.5$ but varying fluctuation amplitude ε (see SM [23] for numerical details). Fig. 2 (C) shows the dependence of λ_1 on ε . The networks produce a negative λ_1 for sufficiently small values of the mean input ε . However, as ε increases λ_1 becomes positive, indicating chaotic network dynamics and thus, asymptotic unreliability. To better understand the nature of this chaotic regime, we compute the *Kaplan-Yorke dimension* ($D_{KY} = k + \sum_{i=1}^k \lambda_i / |\lambda_{k+1}|$ where k is the largest integer such that $\sum_{i=1}^k \lambda_i > 0$), which characterizes the strange attractor on which the dynamics evolve. Fig. 2 shows D_{KY}/N as a function of ε , representing the fraction of phase space on which the dynamics are concentrated. Interestingly, even as λ_1 increases with ε , D_{KY}/N eventually decays as ε gets bigger.

We now explore the effects on network outputs.

Spike time reliability: We use a metric R_{spike} which quantifies the similarity of a family of spike trains by measuring the fraction of spikes that are repeated in each train. If all spike trains are identical, $R_{\text{spike}} = 1$ while if all spikes are far enough apart in time, R_{spike} approaches zero. To compute this value, we follow [31] and define cross-trial *spike events* by time windows surrounding peaks in the spike times histogram, obtained from combining filtered spike trains (see raster plots in Fig. 2 (B) and SM [23]). Events that contain a spike from each train are labeled *reliable*, as are the spikes in them.

Using this metric, we compare the spike output of in-

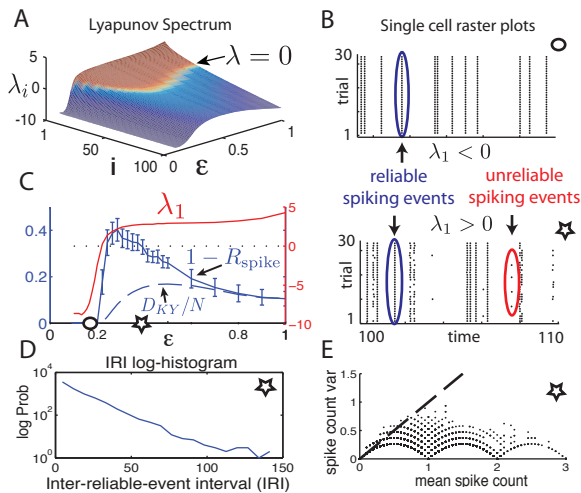


FIG. 2. (A) First 100 Lyapunov exponents of network with parameters as in Fig. 1, as a function of ε . (B) Raster plots show example spike times of an arbitrarily chosen cell in the network on 30 distinct trials, initialized with random ICs. Circle and star markers indicate ε values of 0.18 and 0.45, respectively, shown in panel (C). (C) Multi-scaled plot of λ_1 (right scale), D_{KY}/N and $1 - R_{\text{spike}}$ (left scale) vs ε . Error bars on $1 - R_{\text{spike}}$ curve indicate standard deviation of value across all cells in the network. (D) IRI log histogram (see text) for a sample parameter set (star marker). (E) Variance vs mean for cross-trial single cell spike counts in a time window of width $T=2$ (similar results for different time windows) for a sample parameter set (star marker). Dotted line shows identity (unit Fano factor). For all panels, $\eta = -0.5$.

dividual cells in the network on 30 trials initialized with randomly chosen, network-wide ICs but receiving the same input set $\zeta(t)$. Panel (C) of Fig. 2 shows $1 - R_{\text{spike}}$ versus ε , averaged over every cell in the network. We compute this curve using 2500 time unit runs, discarding the initial 10% to avoid transient effects. As expected, parameter regions where $\lambda_1 < 0$ correspond to $R_{\text{spike}} = 1$ while if $\lambda_1 > 0$ (the chaotic regime), $R_{\text{spike}} < 1$.

However, even if the network is chaotic, R_{spike} remains positive, indicating that many spikes are still reliably repeated across trials. Panel (B) of Fig. 2 illustrates this via raster plots of cross-trial spike times of a randomly chosen cell: even if $\lambda_1 > 0$, the spiking shows repeated temporal structure from trial to trial. The temporal statistics of reliable spike events follow an exponential distribution, as pictured in Fig. 2(D) showing the log histogram of inter-reliable event intervals (IRI). Furthermore, this phenomenon induces cross-trial spike count statistics that further suggest temporal precision: Fig. 2(E) compares the spike count variance and mean, computed across trials in time windows of length $T = 2$. When $\lambda_1 < 0$, the spike count variance is zero as expected (not shown). When $\lambda_1 > 0$, the variance remains generally lower than the mean. This indicates a Fano

factor less than one, thus suggesting spike time precision that substantially exceeds that of the benchmark (inhomogeneous) Poisson process [32].

Importantly, we note that the reliable spike events we observe do not simply follow from choosing the external input amplitude ε to completely dominate all network interactions. Rather, for all parameters explored, network interactions generate larger fluctuations in cell responses than the external input $\varepsilon \zeta_i(t)$ (see SM [23]). Thus the coexistence of chaos and reliable spike events is a dynamical phenomenon, whose origins we now investigate in more detail.

Coexistence of reliable spike events and chaos for $\lambda_1 > 0$: The persistence of reliable spike events in chaotic regimes may be surprising, as one generally expects trajectories to diverge at an exponential rate λ_1 . However, this divergence is confined to lower-dimensional subspaces characterized by the random strange attractor, and is heterogeneous in both time and “space”. We suggest this explains in part the trend in Fig. 2 (B), where $1 - R_{\text{spike}}$ more closely resembles D_{KY}/N than λ_1 .

To better understand the effect of localized space expansion on shorter timescales, we select an example parameter set for asymptotically unreliable dynamics – listed in the caption of Fig. 3– and show that spikes in unreliable events are associated with a greater degree of expansion in the direction of the spiking cells. Consider $v(t)$, the solution of the variational equation $\dot{v} = J(t)v$ where $J(t)$ is the Jacobian of the flow evaluated along the trajectory $\theta(t)$. If we set $v(0)$ to be randomly chosen but with unit length, then $v(t)$ quickly aligns to the directions of maximal expansion in the tangent space of the flow about $\theta(t)$; moreover, $\lambda_1 = \lim_{t \rightarrow \infty} \frac{1}{t} \log(\|v(t)\|)$. We can equivalently write a discretized version of this expression for small Δt : $\lambda_1 = \lim_{T \rightarrow \infty} \langle e(t) \rangle_T$ where $\langle \cdot \rangle_T$ denotes the time average up to time T and $e(t) = \frac{1}{\Delta t} \log \left(\frac{\|v(t+\Delta t)\|}{\|v(t)\|} \right)$ is analogous to a finite time Lyapunov exponent. For our network, $e(t)$ fluctuates rapidly and depends on many factors such as number of spikes fired, the pattern of the inputs, and the phase coordinate of each cell over the time Δt . Its coefficient of variation is typically $\mathcal{O}(10)$ for $\Delta t = 0.005$ which shows that stability is very heterogeneous in time. This further suggests that λ_1 only captures the asymptotic mean of a very wide distribution, giving us little insight into the behavior of the flow on finite timescales.

To better understand the impact of the flow on a single cell’s subspace, we define two quantities

$$s_i(t) = \frac{|v_i(t)|}{\|v(t)\|}$$

$$e_i(t) = \frac{1}{\Delta t} \log \left(\frac{|v_i(t+\Delta t)|}{|v_i(t)|} \right).$$

The *support score* $s_i(t)$ measures the normalized contri-

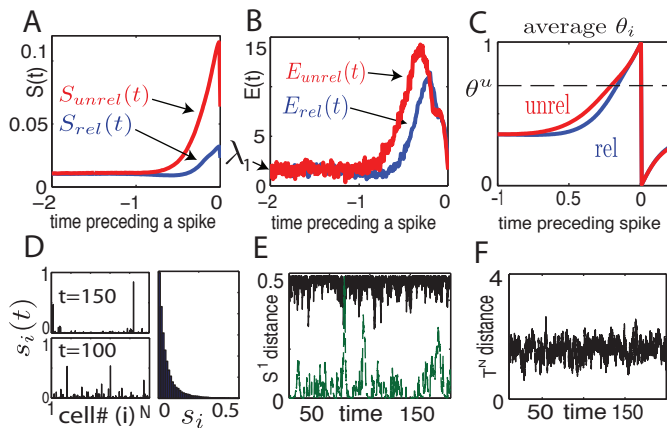


FIG. 3. For (A-C), $t = 0$ marks the spike time and rel/unrel indicate the identity of the spike used in the average. (A) Spike triggered Lyapunov vector support S . (B) Spike triggered local expansion measure E . (C) Spike triggered average phases with unstable fixed point θ^u marking threshold. (D) Left: two snapshots of $s_i(t)$ for different times. Right: histogram of $s_i(t)$ for a randomly chosen cell over a $t = 200$ long trajectory. (E) and (F) Time evolution of distance between two distinct trajectories $\theta^1(t)$, $\theta^2(t)$ (E) Green dashed (bottom): $\|\theta_i^1(t) - \theta_i^2(t)\|_{S^1}$ in randomly chosen θ_i subspace. Black solid (top): $\max_i \{\|\theta_i^1(t) - \theta_i^2(t)\|_{S^1}\}$. (F) $\|\theta^1(t) - \theta^2(t)\|_{T^N}$. Network parameters: $c = 0$, $\eta = -0.5$, $\varepsilon = 0.25$ with $\lambda \approx 1.5$.

bution of a single cell’s subspace to the support of the maximal Lyapunov vector $v(t)$. The *local expansion coefficient* $e_i(t)$ is a local equivalent of $e(t)$. We compare the time course of these two quantities in the moments preceding spikes, by defining the corresponding spike triggered averages $E(t)$ and $S(t)$, i.e., the means of $e_i(t)$ and $s_i(t)$ in a short time interval preceding each spike in the network. We separate reliable spikes from unreliable ones to obtain two versions of both measurements. Fig. 3 shows the resulting averages. Moments before a cell fires an unreliable spike, $S(t)$ is considerably larger than in the reliable spike case, thus indicating that global expansion is further localized in unreliable spike events. Additionally, Fig. 3 (B) shows that $E_{\text{unrel}}(t)$ ’s peak is much broader than $E_{\text{rel}}(t)$ ’s with $\int_{-2}^0 E_{\text{unrel}}(t) - E_{\text{rel}}(t) dt \simeq 2.5$ which indicates that prior to an unreliable spike, trajectories are subject to an accumulated infinitesimal expansion rate higher than in the reliable spike case.

The source of “local” expansion $e_i(t)$ is closely linked to the phase trajectory $\theta_i(t)$ prior to a spike. If $\theta_i(t) < \frac{1}{2}$, the derivative of the single cell flow defined in (1) -in absence of fluctuating inputs (from network or external sources)- is negative, and becomes positive for $\theta_i(t) > \frac{1}{2}$. When an uncoupled cell is driven by ζ_i , we know that on average, it spends more time in its contractive region ($\theta_i < \frac{1}{2}$) and is reliable as a result [13, 20]. While inputs may directly contribute to $J(t)$, their effect is generally so brief that their chief contribution to $e_i(t)$ is to steer

$\theta_i(t)$ in expansive regions of its own subspace. Fig. 3 (C) confirms that the average phase of a cell preceding an unreliable spike spends more time in its expansive region. Such a phenomenon has previously been reported in the form of a threshold crossing velocity argument [33]. We refer the reader to the SM [23] for a detailed treatment of input conditions leading to this phenomenon.

The key feature of this system, likely due to sparse and rapid coupling, is that λ_1 represents a sustained balance between inputs leading to contraction/expansion in local neural subspaces. A bias toward higher frequencies of “expansive inputs” yields $\lambda_1 > 0$ and implies on average more growth than decay in the maximal Lyapunov direction $v(t)$. Because of the local nature of expansive events, this direction is only supported on a few neural directions at a time, as reported in [8] and illustrated in Fig. 3 (D), where we plot snapshots of $v(t)$ ’s components $\{s_i(t)\}_i$. Furthermore, any given cell seldom contributes to $v(t)$ (see s_i histogram in Fig. 3 (D)) which indicates that the identity of subspaces involved in $v(t)$ changes constantly (as also in [8]). This leads to trajectories that are unstable on long timescales ($\lambda_1 > 0$), yet alternate between periods of stability and instability on finite timescales. Fig. 3 (E) shows the time trace of $\|\theta_i^1(t) - \theta_i^2(t)\|_{S^1}$: the projection distance between two randomly initialized trajectories $\theta^1(t)$ and $\theta^2(t)$ in a single cell’s direction as well as $\max_i \{\|\theta_i^1(t) - \theta_i^2(t)\|_{S^1}\}$. While the maximal S^1 distance is almost always close to its maximum 0.5, the two trajectories regularly collapse arbitrarily close in any given S^1 -subspace. In essence, neurons take turns contributing to global separation of trajectories but can become locally stable otherwise. This leads to a global separation $\|\theta^1(t) - \theta^2(t)\|_{T^N}$ that is relatively stable in time (Fig. 3 (F)) yet supports the local, sustained coexistence of reliable and unreliable spike events.

Conclusion: In this Letter, we have explored the reliability of fluctuation-driven networks in the excitable regime –where single cell dynamics contain stable fixed points. Unreliable spikes are a hallmark of sensitivity to initial conditions and may therefore carry information about previous states of the system (or, equivalently, previous inputs). On the other hand, reliable spikes carry repeatable information about the external stimulus $I(t)$ alone. We showed that both unreliable and reliable spike events coexist in chaotic regimes of the system explored. The resulting implications for the neural encoding of signals are an intriguing avenue for future work.

The authors thank Lai-Sang Young for helpful insights. This work was supported in part by an NSERC graduate scholarship, an NIH Training Grant, the Burroughs Wellcome Fund Scientific Interfaces, and the NSF under grant DMS-0907927. Numerical simulations performed on NSF’s XSEDE supercomputing platform.

testage

-
- [1] A. Uchida, R. McAllister, and R. Roy, Physical review letters
- [2] N. Rulkov, M. Sushchik, L. Tsimring, and H. Abarbanel, Physical Review E(1995)
- [3] Y. Shu, A. Hasenstaub, and D. McCormick, Nature **423**, 288 (2003)
- [4] G. Tomko and D. Crapper, Brain Res. **79**, 405 (1974)
- [5] H. Noda and W. Adey, Brain Res. **18**, 513 (1970)
- [6] C. van Vreeswijk and H. Sompolinsky, Neural Comput.(1998)
- [7] M. N. Shadlen and W. T. Newsome, J. Neurosci. **18**, 3870 (1998)
- [8] M. Monteforte and F. Wolf, Phys. Rev. Lett. **105**, 268104 (2010)
- [9] M. London, A. Roth, L. Beeren, M. Häusser, and P. E. Latham, Nature **466**, 123 (2010)
- [10] L. Molgedey, J. Schuchhardt, and H. G. Schuster, Phys. Rev. Lett. **69**, 3717 (1992)
- [11] A. Banerjee, P. Seriès, and A. Pouget, Neural Comput. **20**, 974 (2008)
- [12] K. Rajan, L. Abbott, H. Sompolinsky, and D. Proment, Phys. Rev. E(2010)
- [13] K. Lin, E. Shea-Brown, and L.-S. Young, J. Nonlin. Sci. **19(5)**, 497 (2009)
- [14] K. K. Lin, E. Shea-Brown, and L.-S. Young, J Comput. Neuro. **27**, 135 (Aug 2009)
- [15] A. Litwin-Kumar, A.-M. M. Oswald, N. N. Urban, and B. Doiron, PLoS Comput. Biol. **7**, e1002305 (2011)
- [16] M. Bazhenov, N. Rulkov, J.-M. Fellous, and I. Timofeev, Physical Review E **72**, 041903 (Oct 2005)
- [17] B. Ermentrout, Neural Comput. **8**, 979 (1996)
- [18] P. E. Latham, B. J. Richmond, P. G. Nelson, and S. Nirenberg, J. Neurophysiol. **83**, 808 (2000)
- [19] B. Ermentrout and D. Terman, Mathematical foundations of neuroscience, Vol. 35 (Springer, Interdisciplinary applied mathematics, 2010) p. 422
- [20] J. Ritt, Phys. Rev. E **68**, 1 (2003)
- [21] Z. Mainen and T. Sejnowski, Science **268**, 1503 (1995)
- [22] H. Bryant and J. Segundo, J. Physiology **260**, 279 (1976)
- [23] Supplemental Materials
- [24] B. Lindner, A. Longtin, and A. Bulsara, Neural Comput. **15**, 1761 (2003)
- [25] A. Destexhe, M. Rudolph, and D. Paré, Nat Rev Neurosci **4**, 739 (Sep 2003)
- [26] Y. LeJan, Ann. Inst. Henri Poincaré **23**, 11 (1987)
- [27] Baxendale, Spatial stochastic processes, Progress in Probability, Springer **19**, 189 (1991)
- [28] F. Ledrappier and L.-S. Young, Probab. Th. and Rel. Fields **80**, 217 (1988)
- [29] A. Namenson, E. Ott, and T. Antonsen, Phy. Rev. E **53**, 2287 (1996)
- [30] J. Eckmann and D. Ruelle, Reviews of modern physics **57**, 617 (1985)
- [31] P. Tiesinga, J.-M. Fellous, and T. J. Sejnowski, Nat Rev Neurosci **9**, 97 (2008)
- [32] R. de Ruyter van Steveninck, G. Lewen, S. Strong, R. Koberle, and W. Bialek, Science **275**, 1805 (1997)
- [33] A. Banerjee, J. Comp. Neuro. **20**, 321 (2006)